

Influence of nanoparticle morphology and its dispersion ability regarding thermal properties of water used as Phase Change Material

Camila Barreneche¹, Rosa Mondragon^{2*}, David Ventura-Espinosa³, Jose Mata³, Luisa F. Cabeza⁴, A. Inés Fernández¹, J. Enrique Julia²

¹Department of Materials Science and Physical Chemistry, Universitat de Barcelona, Martí i Franqués 1, 08028-Barcelona, Spain

²Departamento de Ingeniería Mecánica y Construcción, Universitat Jaume I, 12071-Castellon de la Plana, Spain

³Departamento de Química Inorgánica y Orgánica, Universitat Jaume I, 12071-Castellon de la Plana, Spain

⁴GREC Innovació Concurrent, Universitat de Lleida, Edifici CREA, 25001-Lleida, Spain

*Corresponding author: mondrag@uji.es

Tel. +34 964 72 81 45 - Fax +34 964 72 81 06

Abstract

Nanoparticles with different morphologies were added to water to study if the morphology of the nanoparticles affects the main parameters of water used as phase change material (PCM). Considered morphologies were spherical, tubes and sheets in the form of spherical carbon black nanoparticles (CB), multiwalled carbon nanotubes (MWCNT), and graphene oxide nanosheets (GO). Results demonstrate that effectively the morphology of nanoparticles affect the thermophysical properties of the nano-enhanced PCM (NePCM). Depending on the morphology of the added nanoparticle, the final NePCM will have different subcooling and thermal conductivity, whereas its phase change enthalpy is not affected and, therefore, is the same for all produced NePCM.

Keywords: Phase Change Material; nanoparticles; morphology; dispersion; water.

1. Introduction

37 One of the conclusions reached in the 2010 United Nations Climate Change Conference was that
38 Global Warming cannot be avoided, only mitigated [1]. To achieve this objective, efforts should focus
39 on limiting the rise in global temperatures to 2 °C by 2100. In 2015, the Paris Agreement [2] it was
40 established that the 2 °C reduction target was insufficient, and that a 1.5 °C target is required. To meet
41 this goal, the emissions levels for 2030 are 55 GtCO₂e.

42

43 At the current pace of demography and with emerging economies consuming a steadily increasing
44 amount of products and services [3,4], reducing CO₂ emissions relies undoubtedly on innovations in
45 energy technologies to cover energy efficiency, energy harvesting, energy storage, and energy
46 transmission and distribution [5]. These innovations depend on intensifying Research and
47 Development (R&D) activities in forthcoming years to develop an innovative key that enables
48 advanced heat transfer and energy storage materials with market uptake in the mid and long term.

49

50 Energy storage technologies can bridge temporal and geographical gaps between energy demand and
51 supply [6]. Energy storage technologies can be implemented on large and small scales in distributed
52 and centralized manners throughout the energy system. While some energy storage technologies are
53 mature, most of them are still in the early stages of development and additional research efforts are
54 needed. The development of affordable thermal energy storage (TES) technologies will improve the
55 efficiency in the use of energy system resources, increase the use of variable renewable resources of
56 energy, raise the self-consumption and self-production of energy, increase energy access (off-grid
57 electrification), improve the electricity grid stability, reliability and resilience, and increase end-use
58 sector of electrification (e.g. electrification of transport sector). Cold TES is an energy saving
59 technology that reduces the electricity peak by storing cold during off peak hours and in seasonal
60 storage [7,8].

61

62 TES technologies face some barriers to market entry and in this regard cost is a key issue [9,10]. Cost
63 estimates of TES systems include storage media, system (containers, insulation, heat exchanger, and
64 technical equipment for charging and discharging), and operation costs.

65

66 Phase change materials (PCM) can offer high storage capacity associated with the latent heat of the
67 phase change [11,12]. PCM also enable a target-oriented discharging temperature that is set by the
68 constant temperature of the phase change. In addition, in thermal energy storage applications PCM are
69 static, so modular systems ranging from few kW to MW are feasible. However, PCM are not always
70 stable and the boundary conditions of the final application must be controlled [12].

71

72 One of the most promising approaches to improve PCM properties/behaviour is the addition of well-
73 dispersed nanoparticles [13]. In this case, the PCMs are called nanostructured-enhanced phase change

74 materials (NePCM). Nanoparticles can reduce some of the above mentioned drawbacks, but the two
75 most promising to be reduced are low thermal conductivity and high subcooling, since the particles
76 added have higher thermal conductivity and they can act as nucleation points during the phase change.

77

78 Most NePCM studies have used water, etilenglicol, paraffin wax, and cyclohexane as the base PCM
79 [13,14], most of them for cold storage. Different types of nanoparticles have been used including
80 carbon-based nanostructures (carbon nanofibres, graphite nanoplatelets, singlewalled nanotubes, and
81 multiwalled nanotubes, graphne), oxide-based nanoparticles (Al_2O_3 , MgO , TiO_2 , and CuO), and
82 metals (Cu, Al, and Ag) [13,15-17]. In some cases, additives were used to improve nanoparticle
83 dispersion and stability [13,18].

84

85 The last studies revealed that when grafted multi-walled nanotube (MWNT) are introduced in
86 paraffin-montmorillonite composite PCM, paraffin molecules are intercalated in the montmorillonite
87 layers and the grafted MWNTs are dispersed by decreasing the latent heat following the mixture rule
88 and increasing 34% the thermal conductivity [19]. Pissello et al. introduced nanoparticles in cement-
89 based composites encouraging results in terms of added functional properties as electrical conductivity
90 and self-sensing potential for a variety of field scopes, e.g. vibration measurements, damage detection,
91 structural health monitoring, electromagnetic shielding, self-heating pavements for deicing and more
92 [20]. In addition, Karaipekli et al. [21] used a perlite matrix where paraffin PCM was impregnated and
93 nanoparticles were added in order to improve the thermal conductivity and results show up to 25%
94 increment and proper durability and reliability.

95

96 As expected, in most cases, the latent heat of NePCM is lowered because of the presence of solid
97 nanoparticles. Although the rule of mixtures can be used to predict the latent heat in most cases [22],
98 some papers report a reduction in the latent heat even below than the one expected by the rules of
99 mixtures [23]. On the other hand, the addition of nanoparticles to PCM can show a strong influence on
100 the fusion temperature. In most of the studies published to date, a noticeable reduction in the fusion
101 temperature is observed. This reduction is due to a PCM-nanoparticle surface interaction [24].
102 However, some authors report no change in phase change temperature [25-26]. In all the studies, a
103 reduction in the degree of subcooling is observed in NePCM.

104

105 But one of the parameters to consider when adding nanoparticles to a PCM is which
106 material/nanoparticle to use and in which morphology, and this has not been clearly studied in the
107 literature so far. The aim of this paper is to investigate if the different morphology of nanoparticles
108 affects the main parameters of the nanofluid when added to a PCM, mainly its dispersion ability.
109 Therefore carbon based nanoparticles with different morphologies (nanoparticles, nanotubes and
110 nanosheets) were added into water to investigate the effect on this PCM. Other parameters that are

111 also influenced by the addition of nanoparticles in water as PCM were also tested, such as the
112 influence in the melting enthalpy, thermal conductivity and subcooling. The shape and size of the
113 nanostructures are important in a way that the surface to volume ratio of nanostructure alters the
114 thermo-physical properties of the PCM [27].

115

116 **2. Materials and methods**

117

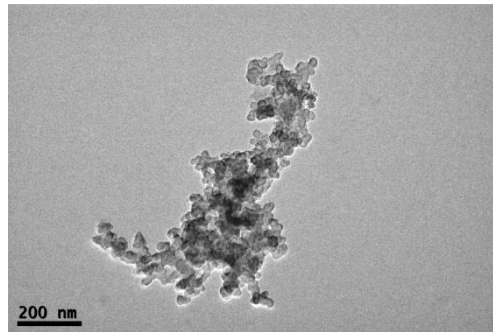
118 Water was doped with three different carbon-based nanoparticles:

- 119 - Spherical carbon black nanoparticles, CB, were supplied by Cabot Corporation. Commercial
120 nanoparticles ELFTEX 570 consist in amorphous carbon with a primary particle size (dp) of
121 10 nm.
- 122 - Multi-walled carbon nanotubes, MWCNT, were purchased from Nanocyl SA. Commercial
123 nanotubes NC7000 present a dp of 9.5 nm and a length of 1.5 μm .
- 124 - Graphene oxide nanosheets, GO, were prepared from graphite powder (natural, universal
125 grade, 200 mesh, 99.9995 %) by the Hummers method and were exfoliated using ultrasounds
126 [28]. Final achieved size was 2 nm in diameter and 1 μm in length.

127 In Figure 1 TEM images of the primary nanoparticles are shown.

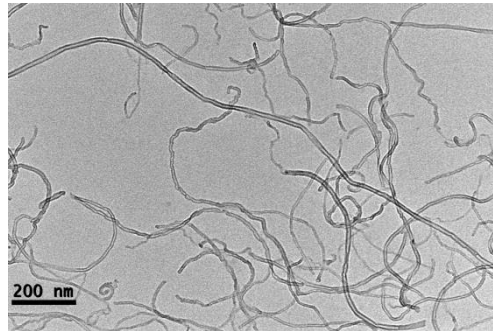
128

129
130



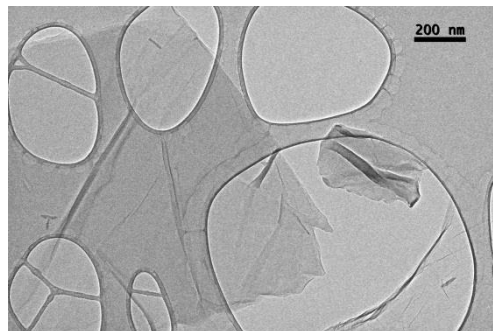
(a)

131
132



(b)

133
134



(c)

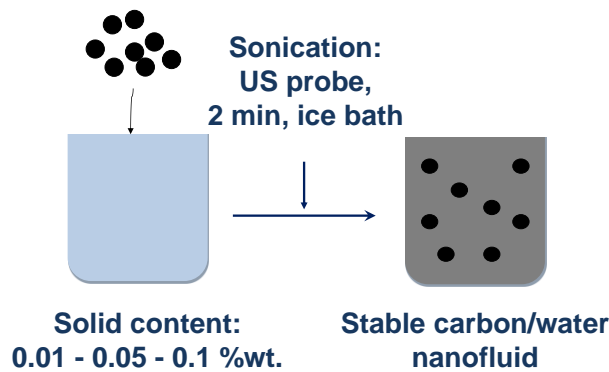
135

Figure 1. (a) Carbon black, (b) MWCNT, (c) graphene oxide nanosheets

136
137
138
139
140
141
142
143
144
145
146

Before the dispersion of the nanoparticles in water, both CB and MWCNT needed to be oxidized with hydrogen peroxide at 120 °C under magnetic stirring to ensure a good dispersion [29]. Finally, carbon-water NePCM were prepared by introducing the corresponding amount of solid into the water. Three solid mass content (0.01% wt., 0.05% wt., and 0.1% wt.) were tested. The breakage of the agglomerates and the dispersion was achieved by means of a sonication treatment with an ultrasound probe, for 2 minutes at low input energy (15%) in an ice bath to avoid heating of the sample (Figure 2). Ultrasound probes provide the highest degree of dispersion; however the breakage of the agglomerates into primary particles is not ensured. Therefore the final size is the lowest it can be obtained under this conditions but nanoparticles are still agglomerate as it can be observed in the results section. With the aim of comparing the different morphologies, it is important to ensure that all the samples are submitted to the same processing and that they were kept stable although there were

147 clusters of primary nanoparticles. In this case samples were checked to be stable and the clusters
148 present did not settle over time.
149



150

151

Figure 2. Preparation of the nanocomposite: nanoparticles + PCM

152

153 The nanoparticles dispersion was characterized by means of the Dynamic Light Scattering (DLS)
154 technique using a ZetaSizer Nano ZS (Malvern Instruments Ltd.). The size distribution of the
155 nanoparticles and agglomerates was obtained for all the samples.

156

157 The phase change enthalpy, temperature and the subcooling reduction were measured by Differential
158 Scanning Calorimetry (DSC) using a DSC2 (Mettler Toledo International Inc.). Approximately 20 mg
159 of sample were introduced in an aluminium crucible sealed in order to avoid loss of material. Samples
160 were submitted to the following cycle: isothermal stage 5 minutes at 20 °C, cooling from 20 °C to -25
161 °C at a cooling rate of 20 °C·min⁻¹, isothermal stage 5 minutes at -25 °C, and heating from -25 °C to 20
162 °C at a heating rate of 20 °C·min⁻¹. Three tests were run for each sample and a mean value was
163 obtained.

164

165 Moreover, the thermal conductivity differences between the samples under study were measured by a
166 hot-wire KD2 Pro thermal analyser device using a transient line heat source method [30] to measure
167 effective thermal conductivity. In this method, a thin metallic wire is embedded in the test liquid
168 acting both as heat source and temperature sensor. The transient hot wire technique works by
169 measuring the temperature/time response of the wire to an abrupt electrical pulse. The sample was
170 introduced in a sealed glass tube (20mL) where the sensor was inserted vertically. Measurements were
171 carried out in solid and liquid phase and the tube was immersed in a thermostatic bath with controlled
172 temperature. Eight measurements were performed for each sample, so the experimental error could be
173 determined at 95% of confidence level.

174

175

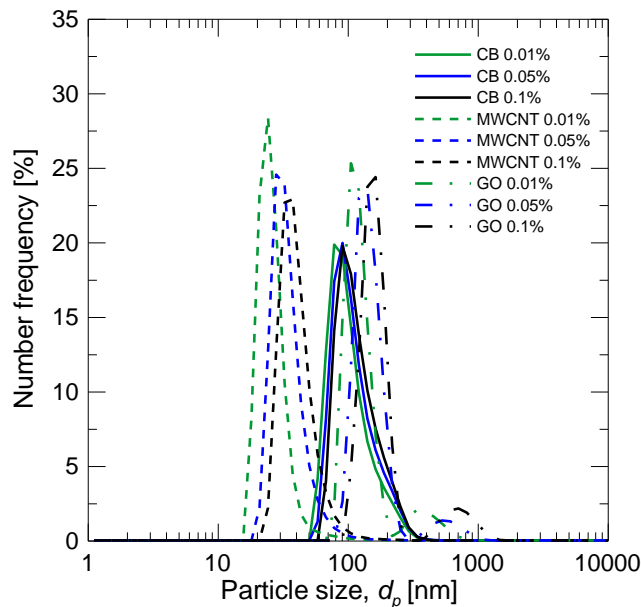
176

177 **3. Results**

178

179 Results related with particles size of nanoparticles and nanoparticles clusters are shown in Figure 3.
180 Figure 3 shows the dispersion of the nanoparticles in the different NePCM measured by the DLS. The
181 dispersion of nanoparticles provides information about the available surface area of the nanoparticles
182 inside the PCM. The NePCM based on CB presented agglomeration, so the average size of the CB
183 clusters, assuming spherical shape, is measured. CB nanoparticles dispersion showed almost no
184 dependence with solid mass content and the cluster average values was similar to those found in other
185 experiments [31]. In the case of NePCM based on GO and MWCNT, the results obtained by the DLS
186 were not so conclusive since the primary nanoparticle morphology was not spherical, and the
187 nanoparticle clusters, if present, neither. Consequently, DLS only provided a rough approximation of
188 the nanoparticle dispersion in non-spherical morphologies. It is possible to observe that by using
189 MWCNT better nanoparticle dispersion is achieved than by using GO nanosheets. This fact limits the
190 available nanoparticle surface area in the case of GO-based nanofluids. Differences found in the
191 agglomeration of nanoparticles of different morphologies depend also on the interparticle interactions
192 due to the surface charges that appear in the nanoparticle surface when they are introduced in water. In
193 the GO-based nanofluids attraction forces seem to be higher providing bigger agglomerates in water.

194



195

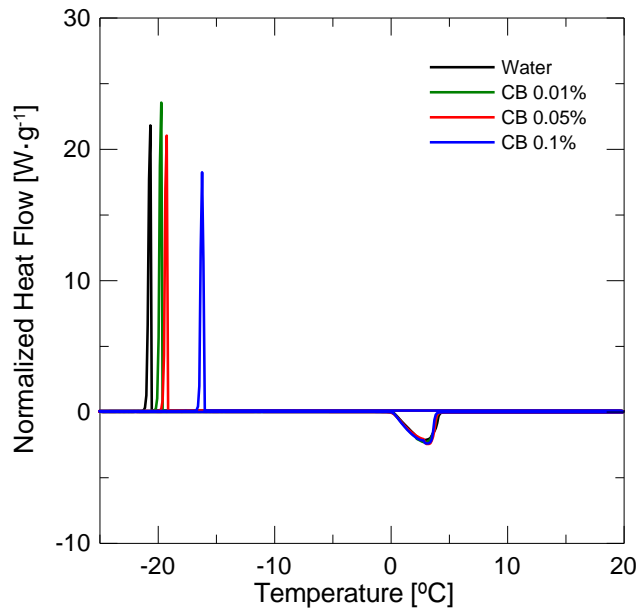
196 **Figure 3. Nanoparticle dispersion degree measured by DLS.**

197

198 Moreover, it is remarkable that after the same sonication process, the different morphologies studied
199 provide also a different degree of agglomeration. All particle size averages obtained have higher
200 values than those reported for the nanoparticles by themselves with cluster sizes bigger than the nano-
201 scale range, depending on the sample. Differences obtained later in the thermal properties analyzed are
202 mainly due to this cluster formation and the available surface area for each material.

203
204
205
206
207
208

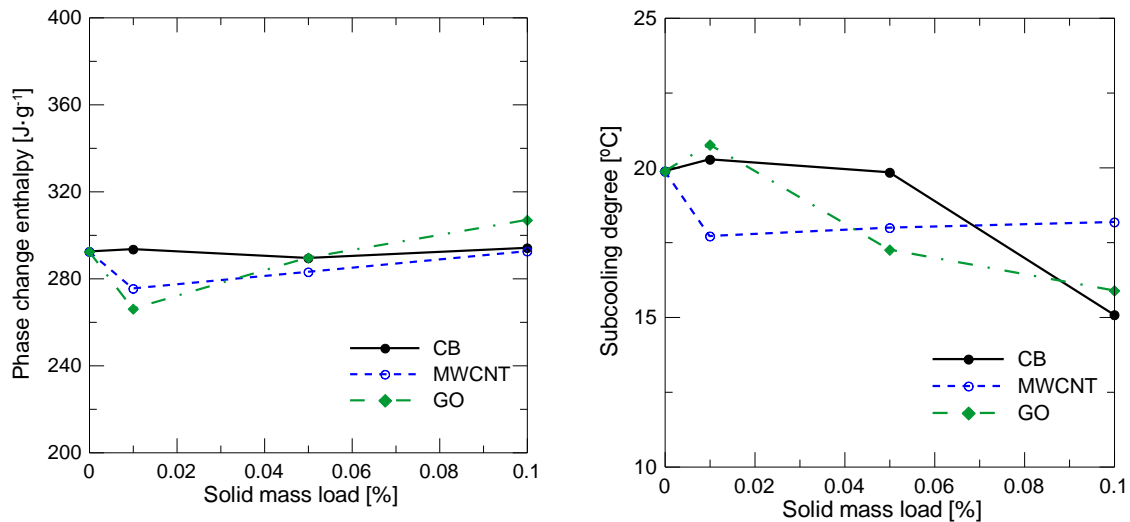
Otherwise, Figure 4 shows the DSC curves for the NePCM based on CB with different solid mass content. It is possible to observe that there was no noticeable dependence of the melting temperature and phase change enthalpy with the nanoparticle mass content. However, a drastic reduction in the subcooling degree of the NePCM when the nanoparticles content is incremented was observed.



209
210
211

Figure 4. DSC curves of NePCM based on CB

212 In order to compare the effect of the different nanoparticle morphologies, Figure 5 shows the phase
213 change enthalpy and subcooling of all the NePCM tested. It is possible to observe that the phase
214 change enthalpy value was almost constant for all the NePCM tested, with values close to the one
215 obtained for the base fluid. However, the subcooling degree depends on the nanoparticle morphology.
216 In the case of CB, it is necessary to use a minimum amount of 0.1% wt. of nanoparticles to get a
217 measurable reduction of subcooling. The maximum reduction of the subcooling for CB is 5 °C. The
218 maximum reduction of subcooling for MWCNT was only 2.5 °C, and it was obtained for low solid
219 mass content (0.01% wt.). The reduction of the subcooling with the nanoparticle amount is almost
220 linear for the GO nanosheets with a maximum decrement of 4 °C.
221



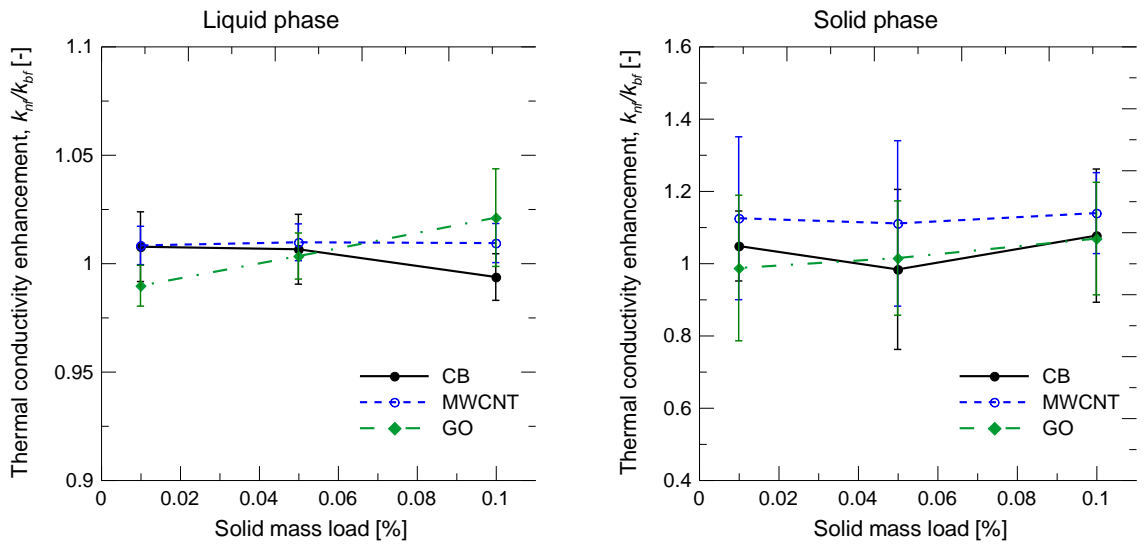
222 **Figure 5. Left: Phase change enthalpy dependence with nanoparticle morphology and solid mass**
 223 **content. Righth: Subcooling degree dependence with nanoparticle morphology and solid mass**
 224 **content.**
 225

226 The addition of solid particles with higher thermal conductivity than the base fluid results in a thermal
 227 conductivity enhancement that can be predicted by the Maxwell equation [32]. However, according to
 228 Gao et al. [33], the enhancement achieved also depends on the size and shape of the particles and
 229 clusters of particles in the nanofluid, and deviations from the Maxwell equation results can be found.
 230

231 The thermal conductivity enhancement measured for the samples under study and its error is shown in
 232 Figure 6. Although a general trend of thermal conductivity increment with solid content can be
 233 observed, it should be noticed that, as the nanofluids tested have a low particle concentration, the
 234 enhancement achieved in liquid phase is negligible for dilute samples. Moreover, for low viscosity
 235 fluids the experimental error increases, and the values obtained for thermal conductivity lie within the
 236 experimental uncertainty. Only for the highest concentration (0.1% wt.) a maximum enhancement of
 237 2.1% can be found for GO nanofluids. It can be also concluded that in liquid phase, the morphology of
 238 the nanoparticles influences the thermal conductivity. For 0.1% wt. solid mass content, nanosheets
 239 (GO) present higher conductivity than nanotubes (MWCNT), while the lower value corresponds to
 240 spherical nanoparticles (CB). The thermal conductivity enhancement and the morphology dependence
 241 measured is in agreement with well established equations [32-33].
 242

243 In solid state, after the phase change, crystallization of water produces a change in the nanoparticle
 244 cluster structure. Therefore, the thermal conductivity depends on the cluster size and its morphology,
 245 which is expected to be different from the primary particles. Consequently, the formation of clusters of
 246 nanoparticles also increases the conduction pathway providing higher enhancements than in liquid

247 phase. In this case, clusters of nanotubes (MWCNT) are the ones with the highest conductivity
 248 enhancement, 13.9%.
 249



250
 251 **Figure 6. Thermal conductivity enhancement. Left: Liquid phase. Right: Solid phase.**

252
 253 As a general rule the thermal properties depend always on the final size of the agglomerates of
 254 nanoparticles. However, for very dilute nanofluids where the interaction among clusters is reduced the
 255 influence of the presence of nanoparticles suspended in the base fluid is negligible and independent on
 256 the particle geometry. Therefore, only for nanofluids in liquid phase at 0.1% of solid mass load
 257 evidences of enhancement of the thermal behaviour can be observed. Otherwise, in solid phase where
 258 nanoparticles agglomerate even more during the phase change the influence of the morphology
 259 becomes important and nanotubes present the higher increase at any concentration due to the high
 260 aspect ratio and the better pathway provided for the transport of phonons responsible for the thermal
 261 conductivity enhancement. Moreover, some theoretical models found in the literature to predict this
 262 enhancement were modified to include the effect of the higher aspect ratio and are valid only for
 263 nanotubes [34].

264
 265 **4. Discussion**

266
 267 Comparing the results obtained in this paper, there are some important highlights detailed as follows:

- 268 - **CB** presented agglomeration, but **size** showed almost **no dependence with solid mass**
 269 **content**. It is possible to obtain a **better nanoparticle dispersion using MWCNT than GO**
 270 nanosheets.
- 271 - There is **no noticeable dependence of the melting temperature** and phase change enthalpy
 272 of the PCM with the nanoparticle mass content.
- 273 - **Subcooling** depends on the nanoparticle morphology:

- 274 • **CB:** it is necessary to use a minimum amount of 0.1% wt. nanoparticles to get a
- 275 measurable reduction of subcooling. The maximum reduction achieved is **5°C**.
- 276 • **MWCNT:** The maximum reduction of subcooling is only **2.5°C**, and it is obtained for
- 277 low solid mass content (0.01% wt.).
- 278 • **GO nanosheets:** The reduction of subcooling with the nanoparticle content is almost
- 279 linear with a maximum decrement of **4°C**.
- 280 - The **phase change enthalpy** is **almost constant** for all the NePCM tested.
- 281 - The **thermal conductivity increment** in solid state is higher when MWCNT nanoparticles are
- 282 used.

283 Based on the results presented in this paper, Table 1 summarized the results obtained with NePCM
 284 containing 0.1% wt. nanoparticles.

285
 286 **Table 1. Summary of results obtained for 0.1% wt. NePCMs tested**

Nanoparticles type	Particle size [nm]	Phase change enthalpy [kJ·kg ⁻¹]	Subcooling reduction [°C]	Thermal conductivity increment (solid) [%]
CB	100	291	5	7.6
MWCNT	35	290	2.5	13.9
GO	110	308	4	6.8

287

288

289 5. Conclusions

290

291 Different morphologies of nanoparticles were used to study if this fact affects the main parameters of
 292 the NePCM when these nanoparticles (CB, MWCNT, and GO) are added to water used as PCM.

293 Results shows that:

- 294 - CB/H₂O NePCM agglomerated when it was put in contact with water, the water phase change
- 295 enthalpy decreased slightly and it had 5 °C of subcooling reduction (the highest obtained in
- 296 this study). The thermal conductivity in solid phase increased almost 8% in solid.
- 297 - MWCNT/H₂O presented the lowest degree of agglomeration when these nanoparticles were
- 298 put in contact with water, water phase change enthalpy remained almost equal and it had the
- 299 lowest subcooling reduction (2.5 °C). Finally, the thermal conductivity measured showed the
- 300 highest increment, around 14% in solid phase by the MWCNT addition.
- 301 - GO/H₂O presented agglomeration when GO nanoparticles were put in contact with water,
- 302 phase change enthalpy was almost not affected by the nanoparticles addition and the phase
- 303 change presented 4 °C of subcooling reduction. The thermal conductivity increased almost 7
- 304 % in solid phase.

305 Therefore, the morphology of the nanoparticles affects the NePCM thermophysical properties and this
306 fact must be taken into account when researchers are producing new NePCM.

307

308 To sum up, the nanoparticles type used will change the agglomerate sizes (notice that MWCNT and
309 GO are not spherical and this issue add an uncertainty to the obtained value); the larger the
310 agglomerate, the higher the subcooling reduction taking into account the subcooling decrement. In
311 addition thermal conductivity enhancement also depends on the morphology of the nanoparticles and
312 the clusters formed during the phase change, providing higher values in solid phase. Finally, the phase
313 change enthalpy for dilute nanofluids is fairly affected by the addition of nanoparticles and can be
314 considered to keep constant.

315

316 **Acknowledgements**

317

318 The research leading to these results has received funding from the European Commission Seventh
319 Framework Programme (FP/2007-2013) under grant agreement n° PIRSES-GA-2013-610692
320 (INNOSTORAGE) and from the European Union's Horizon 2020 research and innovation program
321 under grant agreement No 657466 (INPATH-TES). The authors would like to thank the Catalan
322 Government for the quality accreditation given to their research groups GREA (2014 SGR 123),
323 DIOPMA (2014 SGR 1543). This work has been partially funded by the Spanish government
324 (ENE2015-64117-C5-1-R (MINECO/FEDER) and ENE2015-64117-C5-2-R (MINECO/FEDER)).
325 Dr. Camila Barreneche would like to thank Ministerio de Economía y Competitividad de España for
326 Grant Juan de la Cierva FJCI-2014-22886. This work has been developed by participants of the COST
327 Action CA15119 Overcoming Barriers to Nanofluids Market Uptake (NANOUP TAKE).

328

329 **References**

330

- 331 1. CFR.org "The Global Climate Change Regime". Council on Foreign Relations, 21 July 2012.
332 Web. 16 Feb. 2016.
- 333 2. Sutter, John D.; Berlinger, Joshua (12 December 2015). "Final draft of climate deal formally
334 accepted in Paris". CNN. Cable News Network, Turner Broadcasting System, Inc. Retrieved 12
335 December 2015.
- 336 3. Cabeza, L.F., Urge-Vorsatz, D., McNeil, M.A., Barreneche, C., Serrano, S. Investigating
337 greenhouse challenge from growing trends of electricity consumption through home appliances in
338 buildings. 2014. Renewable and Sustainable Energy Reviews 36, 188-193.
- 339 4. Üрге-Vorsatz, D., Cabeza, L.F., Serrano, S., Barreneche, C., Petrichenko, K. Heating and cooling
340 energy trends and drivers in buildings. 2015. Renewable and Sustainable Energy Reviews 41, 85-
341 98.

- 342 5. EUROPEAN COMMISSION. 2015. A Framework Strategy for a Resilient Energy Union with a
343 Forward-Looking Climate Change Policy.
- 344 6. S. Kalaiselvam, R. Parameshwaran. Thermal Energy Storage Technologies for Sustainability:
345 Systems Design, Assessment and Applications. Elsevier, USA. ISBN: 978-0-12-417291-3. 2014.
- 346 7. Oró, E., de Gracia, A., Castell, A., Farid, M.M., Cabeza, L.F. Review on phase change materials
347 (PCMs) for cold thermal energy storage applications. 2012. Applied Energy 99, 513-533.
- 348 8. Veerakumar, C., Sreekumar, A. Phase change material based cold thermal energy storage:
349 Materials, techniques and applications - A review. 2016. International Journal of Refrigeration 67,
350 271-289.
- 351 9. IEA-ETSAP, IRENA. Thermal Energy Storage - Technology Brief E17. 2013. Available from:
352 [https://www.irena.org/DocumentDownloads/Publications/IRENA-](https://www.irena.org/DocumentDownloads/Publications/IRENA-ETSAP%20Tech%20Brief%20E17%20Thermal%20Energy%20Storage.pdf)
353 [ETSAP%20Tech%20Brief%20E17%20Thermal%20Energy%20Storage.pdf](https://www.irena.org/DocumentDownloads/Publications/IRENA-ETSAP%20Tech%20Brief%20E17%20Thermal%20Energy%20Storage.pdf) (16/02/2016)
- 354 10. SHC-Task 42, ECES-Annex 29. Compact Thermal Energy Storage IEA SHC Position Paper.
355 2015. Available from: [https://www.iea-shc.org/data/sites/1/publications/IEA-SHC-Compact-](https://www.iea-shc.org/data/sites/1/publications/IEA-SHC-Compact-Thermal-Storage-Position-Paper.pdf)
356 [Thermal-Storage-Position-Paper.pdf](https://www.iea-shc.org/data/sites/1/publications/IEA-SHC-Compact-Thermal-Storage-Position-Paper.pdf) (16/02/2016).
- 357 11. Farid, M.M., Khudhair, A.M., Razack, S.A.K., Al-Hallaj, S. A review on phase change energy
358 storage: Materials and applications. 2004. Energy Conversion and Management 45 (9-10), 1597-
359 1615.
- 360 12. Cabeza, L.F., Castell, A., Barreneche, C., De Gracia, A., Fernández, A.I. Materials used as PCM
361 in thermal energy storage in buildings: A review. 2011 Renewable and Sustainable Energy
362 Reviews 15 (3), 1675-1695.
- 363 13. Kaviarasu, C., Prakash, D. Review on phase change materials with nanoparticle in engineering
364 applications. 2016. Journal of Engineering Science and Technology Review 9 (4), 26-386.
- 365 14. Mondragón R., Martínez-Cuenca R., Hernández L., Andreu-Cabedo P., Cabedo L., Julià J.E.
366 Handbook of Clean Energy Systems, Volume 5 - Energy Storage: Thermal Energy Storage;
367 Chemical Storage; Mechanical Storage; Electrochemical Storage; Integrated Storage Systems.
368 Chapter 33 – Nanotechnology and Nanomaterials for thermal energy storage. Editor-in-chief:
369 Jinyue Yan. Wiley, UK, 2015. ISBN: 978-1-118-38858-7.
- 370 15. Li, Y., Zhou, J., Tung, S., Schneider, E., Xi, S. A review on development of nanofluid preparation
371 and characterization. 2009. Powder Technology 196 (2), 89-101.
- 372 16. Sidik, N.A.C., Mohammed, H.A., Alawi, O.A., Samion, S. A review on hybrid nanofluids: Recent
373 research, development and applications. 2014. International Communications in Heat and Mass
374 Transfer 54, 115-125.
- 375 17. Sathishkumar, A., Kumaresan, V., Velraj, R. Solidification characteristics of water based graphene
376 nanofluid PCM in a spherical capsule for cool thermal energy storage applications. 2016.
377 International Journal of Refrigeration 66, 73-83.

- 378 18. Wang, J., Xie, H., and Xin, Z. Thermal properties of heat storage composites containing
379 multiwalled carbon nanotubes. 2008. *Journal of Applied Physics* 104, 113537–113545.
- 380 19. Li, M., Guo, Q., Nutt, S. 2017. Carbon nanotube/paraffin/montmorillonite composite phase
381 change material for thermal energy storage. *Solar Energy* 146, 1–7.
- 382 20. Pisello, A.L., D’Alessandro, A., Sambuco, S., Rallinic, M., Ubertinia, F., Asdrubalia, F.,
383 Materazzic, A.L., Cotana F. 2017. Multipurpose experimental characterization of smart
384 nanocomposite cement-based materials for thermal-energy efficiency and strain-sensing
385 capability. *Solar Energy Materials & Solar Cells* 161, 77–88.
- 386 21. Karaipekli, A., Biçer, A., Sarı, A., Tyagi, V. 2017. Thermal characteristics of expanded
387 perlite/paraffin composite phase change material with enhanced thermal conductivity using carbon
388 nanotubes. *Energy Conversion and Management* 134, 373–381.
- 389 22. Zeng, J.L., Cao, Z., Yang, D.W., et al. Thermal conductivity enhancement of Ag nanowires on an
390 organic phase change material. 2010. *Journal of Thermal Analysis and Calorimetry* 101, 385–389.
- 391 23. Wu, S., Zhu, D., Zhang, X., and Huang, J. Preparation and melting/freezing characteristics of
392 Cu/paraffin nanofluid as phasechange material (PCM). 2010. *Energy and Fuels* 24, 1894–1898.
- 393 24. Hong, H., Wensel, J., Peterson, S., and Roy, W. Efficiently lowering the freezing point in heat
394 transfer coolants using carbon nanotubes. 2007. *Journal of Thermophysics and Heat Transfer* 21,
395 446–448.
- 396 25. Ho, C.J. and Gao, J.Y. Preparation and thermophysical properties of nanoparticle in paraffin
397 emulsion as phase change material. 2009. *International Communications in Heat and Mass*
398 *Transfer* 36, 467–470.
- 399 26. Kumaresan, V., Velraj, R., and Das, S.K. The effect of carbon nanotubes in enhancing the thermal
400 transport properties of PCM during solidification. 2012. *Heat and Mass Transfer* 48, 1345–1355.
- 401 27. Parameshwaran R., Kalaiselvam S.. Nanomaterial-embedded phase-change materials (PCMs) for
402 reducing building cooling needs. 2015. *Eco-efficient Materials for Mitigating Building Cooling*
403 *Needs* 401–443.
- 404 28. Hummers, W. S.; Offeman, R. E. 1958. Preparation of Graphitic Oxide. *Journal of the American*
405 *Chemical Society* 80, 1339-1339.
- 406 29. Han, D.X., Meng, Z.G., Wu, D.X., Zhang, C.Y., Zhu, H.T. Thermal properties of carbon black
407 aqueous nanofluids for solar absorption. 2011. *Nanoscale Research Letters* 6, 457, 1-7.
- 408 30. Mujumdar, A. S. *Handbook of Industrial Drying*. Third Edition 25 (6). CRC Press 2006.
- 409 31. Mondragon, R., Segarra, C., Martinez-Cuenca, R., Julià E, Jarque JC. Experimental
410 characterization and modeling of thermophysical properties of nanofluids at high temperature
411 conditions for heat transfer applications. 2013. *Powder Technology* 249, 516–529.
- 412 32. Maxwell J C. *A Treatise on Electricity and Magnetism* 1873, Clarendon Press Oxford
- 413 33. Gao J W, Zheng R T, Ohtani H, Zhu D S and Chen G. Experimental investigation of heat
414 conduction mechanisms in nanofluids. Clue on clustering. 2009. *Nano Letters* 9 (12) 4128-32.

415 34. Yang, L., Xu, J., Du, K., Zhang, X. 2017. Recent developments on viscosity and thermal
416 conductivity of nanofluids. *Powder Technology* 317, 348–369.